The current issue and full text archive of this journal is available at
www.emeraldinsight.com/0961-5539.htm

Application of axisymmetric analog to unstructured grid for aeroheating prediction of hypersonic vehicles

H. Parhizkar and S.M.H. Karimian
Center of Excellence in Computational Aerospace Engineering, Department of Aerospace Engineering, Amirkabir University of Technology, Tehran, Iran

Received 28 July 2007
Revised 7 April 2008
Accepted 9 April 2008

Abstract

Purpose – The purpose of this paper is to present an engineering inviscid-boundary layer method for the calculation of convective heating rates on three-dimensional non-axisymmetric geometries at angle of attack.

Design/methodology/approach – Based on the axisymmetric analog, convective heating rates are calculated along the surface streamlines which are determined using the inviscid properties calculated on an unstructured grid.

Findings – Since the method is capable of using inviscid properties calculated on an unstructured grid, it is applicable to a variety of configurations and it requires much less computational effort than a Navier-Stokes code. The results of the present method are evaluated on different wing body configurations in laminar and turbulent hypersonic equilibrium flows. In comparison to experimental data, the present results are found to be fairly accurate in the windward and leeward regions.

Practical implications – With this approach, heating rates can be predicted on general three-dimensional configurations at hypersonic speeds in an accurate and fast scheme.

Originality/value – In order to calculate the heating rates at any specific point on the surface, a technique is developed to calculate the inviscid surface streamlines in a backward manner using the inviscid velocity components. The metric coefficients are also calculated using a new simple technique.

Keywords Aerodynamics, Heating, Aircraft
Paper type Research paper

Nomenclature

d	average of three cell edge lengths	r	axisymmetric body radius
h	streamline metric coefficient	R	recovery factor
H	enthalpy	R_n	nose radius
M	Mach number	Re	Reynolds number
N	turbulent velocity profile exponent	St	Stanton number
n_1, n_2, n_3	vertices of a triangular cell	s	coordinate along streamline
pr	Prandtl number	T	temperature
P	pressure	u, v, w	surface velocity components in the Cartesian coordinate system
q	surface heat flux	x, y, z	Cartesian coordinate system
		xs, ys, zs	starting point coordinates

The authors are grateful to the Aerospace Department of Amirkabir University of Technology for their financial support.

International Journal of Numerical Methods for Heat & Fluid Flow
Vol. 19 Nos. 3/4, 2009
pp. 501-520

0961-5539
DOI 10.1108/09615530910938407

α	angle of attack
δ	boundary layer thickness
θ	boundary layer momentum thickness
ρ	density
μ	viscosity

Subscripts

aw	adiabatic wall
e	boundary layer edge
ie	surface cell
iv	surface node
L	laminar
T	turbulent
w	wall
∞	free stream condition

1. Introduction

The calculation of aerodynamic heating rates on hypersonic vehicles remains a challenging problem. Such analysis often involves multidimensional geometries with leading-edge bluntness and fuselage-wing combinations with arbitrary cross sections. In addition, at hypersonic flight conditions the dissociation of air at high temperatures and its effects on the surface heating must be taken into account (Anderson, 1989). Numerical simulation of full compressible Navier-Stokes equations for three-dimensional flow fields is still not economic for preliminary design of these vehicles where a range of geometries and flow parameters are to be studied. A review of literature shows that to reduce this huge amount of computational effort, Cooke (1961) developed a simple method for calculation of three-dimensional viscous flow, using axisymmetric analog. Following this approach, the general three-dimensional boundary layer equations are written in a streamline coordinate system having neglected the cross-flow velocity. This reduces the three-dimensional boundary layer equations to a form that is identical to those of axisymmetric flow, provided that the distance along a streamline is interpreted as the distance along an "equivalent body". In addition, the metric coefficient that describes the spreading of streamlines is interpreted as the radius of an equivalent body. This allows the existing axisymmetric boundary layer codes to be used for the calculation of the approximate three dimensional heating rates along a streamline. In lieu of numerically integrating the axisymmetric boundary layer equations, a set of approximate convective-heating equations developed by Zoby *et al.* (1981) is used to even more reduce the computational difficulties and its costs.

In order to apply the axisymmetric analog for computation of heating rates on three-dimensional bodies, the inviscid surface streamlines and the metric coefficients should be calculated. Practically, the most difficult part of applying axisymmetric analog is the computation of inviscid surface streamlines and metric coefficients (DeJarnette *et al.*, 1978). Several investigators (Riley and DeJarnette, 1990, 1991, 1992a, b; Riley, 1992; Riley *et al.*, 1998; Karimian and Mahdizadeh, 2001; Malekzadeh *et al.*, 2003) have used Maslen method (Maslen, 1964, 1971) to calculate approximate inviscid flow field properties, but this method was found to be too complicated to be used in three-dimensional cases (DeJarnette *et al.*, 1978). DeJarnette and Davis (1968) calculated the streamlines emanating from the stagnation point by a fairly simple method. These streamlines are consistent with the Newtonian concept that a fluid particle loses its normal component of momentum upon striking a body surface. DeJarnette and Hamilton (1973) developed a simple method for calculating streamlines from a known pressure distribution. However, this approach is difficult to be applied, unless the

surface geometry and pressures can be described analytically (DeJarnette *et al.*, 1978). More success has been achieved when the streamline information is derived from velocity components on the surface obtained from complete three-dimensional inviscid flowfield calculations (Hamilton *et al.*, 1987, 1993; Parhizkar and Karimian, 2006).

Hamilton *et al.* (1987) developed an engineering method based on the axisymmetric analog for 3-D heating rate calculation. In their approach, heating is calculated along the each individual streamline, starting from its origin at the stagnation point to the end of the body. If this approach is used for a wing-body combination, large regions of the wing surface are often missed and not covered by the selected streamlines (see Figure 1).

Repeating the process of selecting proper starting point for new streamlines to cover the missed regions is a tedious task and mostly not successful. To resolve this problem, Hamilton *et al.* (1993) redistributed the streamlines at some computational steps downstream of the stagnation point. With this approach, Riley predicts aeroheating of X-34 reusable launch vehicle (Riley *et al.*, 1998).

In the previous methods (Riley *et al.*, 1998; DeJarnette and Davis, 1968; DeJarnette and Hamilton, 1973; Hamilton *et al.*, 1987, 1993; Parhizkar and Karimian, 2006), the inviscid streamlines and the streamline metrics were obtained from the inviscid solution calculated on a structured grid. However, inviscid solution can be obtained for more complex geometries, using unstructured grids. As it is reported in Dyakonov and DeJarnette (2003), the application of axisymmetric analog to unstructured grid was started in unfinished research by Riley and DeJarnette. It was in this reference that Dyakonov and DeJarnette used inviscid flow properties obtained from an unstructured grid to calculate streamlines and metric coefficients. But due to the difficulties encountered in the application of their method, their code called UNLATCH were limited to solution of simple blunt cones. It was in the recent paper of Hamilton and DeJarnette (Hamilton *et al.*, 2006) in 2006 that a new code called UNLATCH2 was developed to compute heating rates on more complex configurations using unstructured grids.

In the present work, a new technique is developed to calculate the inviscid surface streamlines and streamline metrics from the inviscid properties calculated on an unstructured grid. The present formulation is completely different from the previous works and less complicated than them and it involves fewer interpolations than them. Started from the specific point on which the heating rate is required, its corresponding streamline is traced backward to its stagnation point. The streamline metrics are calculated from the normal distance between two streamlines at each point. After

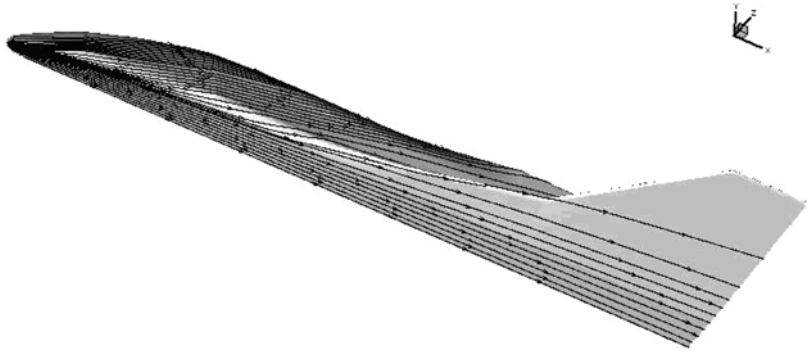

Figure 1.
Surface streamlines starting from stagnation region for a wing-body configuration

determination of the correct streamline for the selected point and metric coefficients, the Zoby's approximate convective heating equations are integrated from the stagnation point along this streamline to yield the aeroheating rate on the started point. The present method is simple and easy to use for computer codes and is capable of computing the laminar and turbulent heating rates on the windward and leeward surfaces of any three dimensional bodies with minimum user intervention.

2. Approximate convective heating equations

The Zoby's approximate convective heating equations (Zoby *et al.*, 1981) are obtained from the integral form of the axisymmetric boundary layer momentum equation (White, 1974). Having applied the reference enthalpy method (Eckert, 1955) (for compressibility effects) and the Reynolds analogy (White, 1974) to the integral form of the momentum equation, the approximate convective heating equations are given below. The equations for laminar flow are as follows (DeJarnette *et al.*, 1978):

$$q_{wL} = 0.22(\mathrm{Re}_{\theta L})^{-1}\left(\frac{\rho^*}{\rho_e}\right)\left(\frac{\mu^*}{\mu_e}\right)\rho_e V_e (H_{aw} - H_w)(pr_w)^{-0.6} \tag{1}$$

The variables of ρ^* and μ^* are introduced to consider the compressibility effects. These variables are evaluated at the Eckert's reference enthalpy (Eckert, 1955) defined as:

$$H^* = 0.50H_e + 0.50H_w + 0.22R\frac{V_e^2}{2} \tag{2}$$

The momentum-thickness Reynolds number is defined as:

$$\mathrm{Re}_{\theta_L} = \frac{\rho_e V_e \theta_L}{\mu_e} \tag{3}$$

In which, θ_L, the laminar boundary layer momentum thickness is:

$$\theta_L = \frac{0.644\left[\int_0^s \rho^*\mu^* V_e r^2 ds\right]^{1/2}}{\rho_e V_e r} \tag{4}$$

The adiabatic wall enthalpy is defined as:

$$H_{aw} = H_e + 0.5RV_e^2 \tag{5}$$

In which the recovery factor is equal to $\mathrm{Pr}^{1/2}$ for laminar flow and equal to $\mathrm{Pr}^{1/3}$ for turbulent flow (White, 1974). Similar equations are developed for the turbulent flow (Zoby *et al.*, 1981):

$$q_{wT} = c_1(\mathrm{Re}_{\theta T})^{-m}\left(\frac{\rho^*}{\rho_e}\right)\left(\frac{\mu^*}{\mu_e}\right)^m \rho_e V_e (H_{aw} - H_w)(pr_w)^{-0.4} \tag{6}$$

$$\theta_T = \frac{c_2\left[\int_0^s \rho^*\mu^{*m} V_e r^{c_3} ds\right]^{c_4}}{\rho_e V_e r} \tag{7}$$

The coefficients of m, c_1, c_2, c_3 and c_4 are functions of N, which is the exponent of the power-law turbulent velocity profile (Zoby *et al.*, 1981), and are given by:

$$\begin{aligned} m &= \frac{2}{N+1} & c_3 &= 1+m \\ c_1 &= \left(\frac{1}{c_5}\right)^{2N/N+1}\left[\frac{N}{(N+1)(N+2)}\right]^m & c_4 &= \frac{1}{c_3} \\ c_2 &= (1+m)c_1 & c_5 &= 2.2433 + 0.93N \end{aligned} \tag{8}$$

A turbulent velocity profile of $V/V_e = (y/\delta)^{1/N}$ is assumed to calculate the required constants and exponents in the equations of momentum-thickness Reynolds number and the convective heat flux. Experimental results (Johnson and Bushnell, 1970) show that N would be a function of Re_{θ_T}. Fitting a curve to the turbulent experimental data (Zoby *et al.*, 1981) produces the following equation:

$$N = 12.67 - 6.5Log(\mathrm{Re}_{\theta T}) + 1.21[Log(\mathrm{Re}_{\theta T})]^2 \tag{9}$$

For the perfect gas model, the viscosity is obtained using the Sutherland formula (White, 1974), and the specific heat ratio and Prandtl number are assumed to be the constant values of 1.4 and 0.71 for air, respectively. The thermal conductivity, however, is obtained from the definition of Prandtl number.

The mixture thermodynamic and transport properties of chemically reacting equilibrium air are provided in the form of tables by Tannehill and Mugge (1974). In this paper enthalpy $H(p, T)$ and density $\rho(p, T)$ are interpolated from the tabular data. However, the transport properties of viscosity and thermal conductivity are interpolated from the tables provided by Hansen (1958). The Prandtl number is calculated using viscosity, thermal conductivity, and the mixture specific heat which obtained by numerical differentiation of enthalpy data. In Simeonides (1998), it has been shown that the Eckert's reference enthalpy formulation (Equation (2)) is still valid for equilibrium air. It should be noted that the values of ρ^* and μ^* must be evaluated at the thermodynamic properties of the Eckert's reference enthalpy (H^*) and the edge pressure (p_e) (Simeonides, 1998).

Having known the values of pressure, temperature and the velocity magnitude at the edge of boundary (i.e. P_e, T_e and V_e) from the inviscid solution, the heating rates can be calculated on the surface of body, from either Equation (1) or (6). This completes the calculation procedure for axisymmetric bodies.

The above equations are derived for attached boundary layer, based on the integral form of the axisymmetric boundary layer equations. Therefore they cannot predict the peak heating which occurs in the vicinity of boundary layer reattachment. In the case of flow separation, full Navier-Stokes equations should be solved around the vehicle (Hillier and Soltani, 1995; Mehta, 2000; Mulas *et al.*, 2002; Soltani *et al.*, 1993).

3. Axisymmetric analog

The laminar flow equations of (1)-(5) and the turbulent flow equations of (6)-(9) are derived for axisymmetric flow. These relations may be applied to 3-D flow using the axisymmetric analog (Zoby *et al.*, 1981) approximation. The axisymmetric analog assumptions allow the axisymmetric boundary layer relations given above to be used in a surface streamline coordinate system provided that the following substitution is

made: $r = h$; where h is the scale factor describing the divergence of the surface streamlines (Zoby *et al.*, 1981).

4. Inviscid surface streamlines

Any unstructured inviscid code can be used in this method to determine the inviscid solution properties on the body surface. The format of data that should be exported to a file include a set of $x_{iv}, y_{iv}, z_{iv}, u_{iv}, v_{iv}, w_{iv}, P_{iv}$ and T_{iv} values for all the surface nodes, and a set of n_{1ie}, n_{2ie} and n_{3ie} for the all of surface cells. We know that surface streamlines emanate from the stagnation region and spread out all over the body surface. It is very difficult to start a streamline path from the stagnation point and have it passed through a specific point on the body surface, on which the heating rate is needed. To resolve this difficulty, a procedure is developed to trace the streamline from the specific point backward to a point very close to the stagnation point. This can be done easily by reversing the sign of velocity components in the above procedure. A reversed process then can be started from the calculated point in the stagnation region to re-trace the streamline toward the specific point while computing heating rates along the streamline.

Here we describe the procedure. Starting from a specific starting point of $p1$(*xs, ys, zs*), three triangles are formed by connecting $p1$ to the three corners of each cell, e.g. n_1, n_2 and n_3 in Figure 2. The starting cell would be the one that its area (S) is equal to the area of these triangles, i.e. as shown in Figure 2, $S = S1 + S2 + S3$.

Streamline direction is equal to the velocity direction at point $p1$. This direction is determined from the linear interpolation of the cell vertex velocities. Second node of the streamline would be the intersection of the streamline and the cell edge. Since the velocity components are obtained from interpolation scheme, the streamline direction would not be exactly tangent to the cell surface when crossing its edges. Therefore, the streamline direction may not intersect any of the cell edges in 3-D space. This problem is resolved by intersecting the projection of streamline direction with the cell edges, as shown in Figure 3. In this figure the coordinates of $p1$ are xs, ys and zs, and $p2$ is located at $xs + u/V * d, ys + v/V * d$ and $zs + w/V * d$. Point $p2$ then is projected on cell (n_1, n_2, n_3) surface to define point $p3$. In this situation, the line connecting p1-p3 surely intersects the cell edge at a point called $p4$. Now the line of $p1 - p4$ would be the streamline passing from point $p1$.

To ensure that the point $p4$ is correctly detected, all intersections between the line of $p1 - p3$ and three edges of cell should be examined. The correct intersection point of $p4$ should meet the following criteria, (a) summation of distance between $p4$ and the two

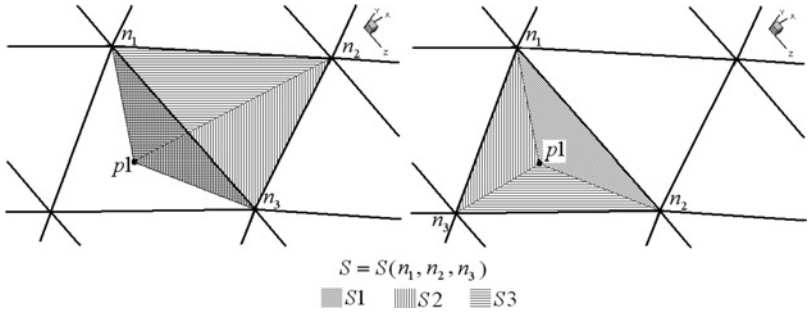

Figure 2.
Determination of the starting cell, Left: $S1 + S2 + S3 > S$ and right: $S1 + S2 + S3 = S$

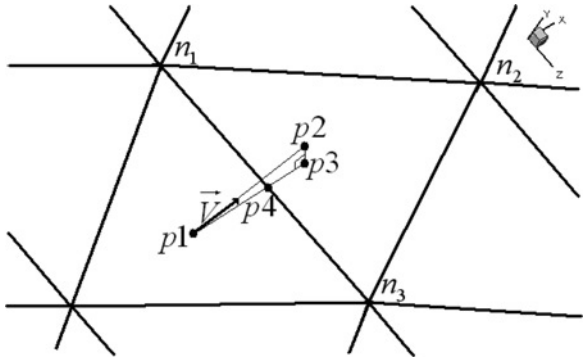

Figure 3.
Streamline tracing points

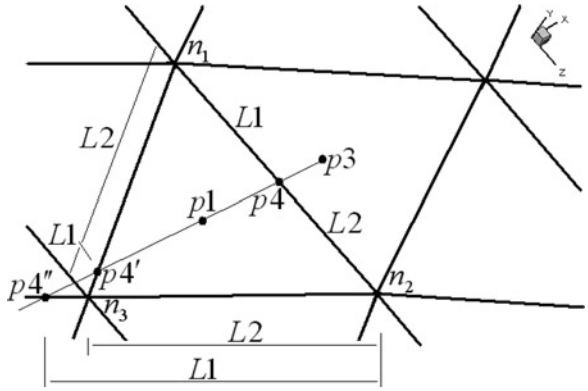

Figure 4.
Intersection between streamline and cell edges

vertices of the corresponding edge is equal to the edge length, i.e. L1 + L2 = L, and (b) s-coordinate of the intersection point is greater than the starting point (Figure 4).

The above procedure is repeated from p4 as the new starting point. The velocity components at this point are interpolated linearly from the velocities at the n_1 and n_2 vertex points. Two comments should be made here, (a) depending on the direction along which streamline is calculated (toward stagnation or toward specific point), the sign of velocity components should be set, and (b) the point very close to the stagnation point in the stagnation region, is determined when the surface slip velocity is less than a very small predefined value.

5. Metric coefficient

The most difficult part of applying axisymmetric analog technique is computing the metric coefficient associated with the spreading of the streamlines. DeJarnette and Hamilton (1973) developed a simple method for computing the streamline metric coefficient from a known surface pressure distribution. The application was limited to simple body shapes. They developed the new method (Hamilton *et al.*, 1987) in 1987 and used surface velocity distribution for calculating metric coefficients on windward surface of space shuttle orbiter. Hamilton *et al.* (1993) modified their method and developed a code called LATCH (Langley Approximate Three-Dimensional Convecting Heating). This code assumes that the inviscid flowfield properties were computed on a single block structured mesh with a generalized body fitted coordinate system. The

application was shuttle orbiter with simplified leeside plane. It was in 1998 that Riley *et al.* (1998) calculate X-34 windward and leeward heating rates using LATCH.

In 2006, Hamilton *et al.* (2006) developed an unstructured version of LATCH called UNLATCH2. In their code, starting with the approximate solution on the epsilon curve around stagnation point, the solution at the grid points at the vertices of the stagnation triangle are computed along with several other grid points in the vicinity of the stagnation point denoted by the grid points enclosed in circles in Figure 5. Next the solution is computed at grid points on both the lower and upper symmetry planes of the body. Once solutions at grid points around the stagnation point and on the symmetry plane have been computed, the solutions at all the other grid points downstream of the stagnation point are performed. Having known the solution at grid points 1 and 2 of the triangular element shown in Figure 6, solution at grid point 3 can be computed. Starting at point 3 the streamline passing through 3 is integrated backwards in space and the point 4 is determined where it intersects the opposite side of the triangle (the line connecting points 1 and 2). The initial conditions at this point including $\partial y/\partial\beta, \partial z/\partial\beta, F_x, F_y, F_z$, u, v, w and θ are computed from the known solutions at points 1 and 2. Then the streamline, metric and heating equations are integrated forward in space to complete the solution at point 3. The derived formula for calculating streamline metric in Hamilton *et al.* (2006) is:

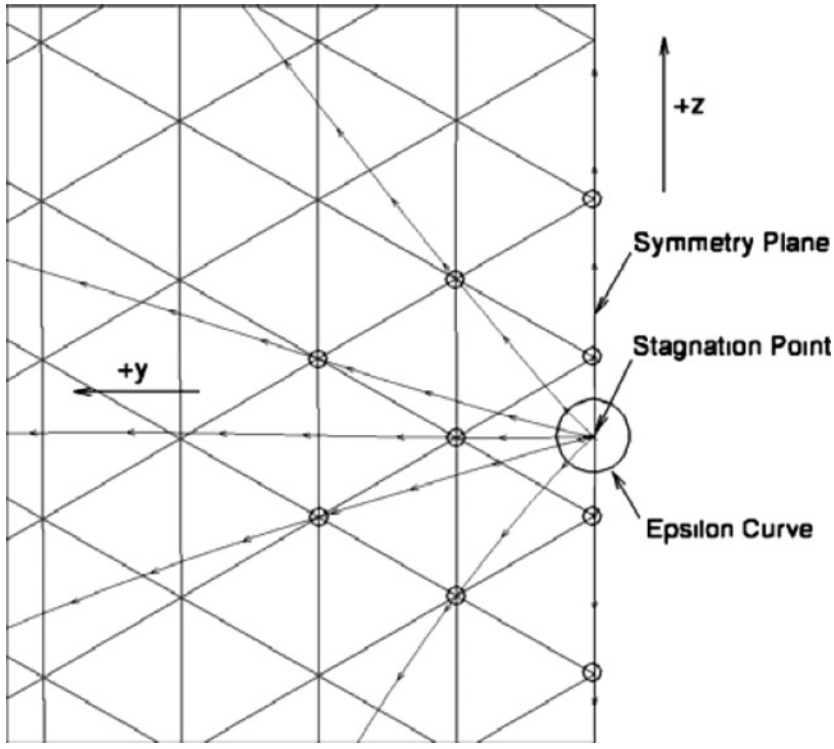

Figure 5.
Solution strategy of UNLATCH2 at grid points in stagnation region

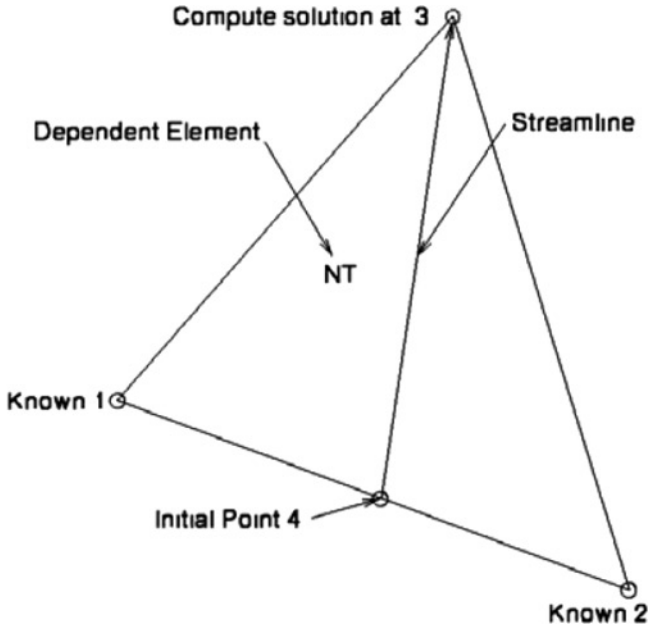

Figure 6.
Solution strategy of UNLATCH2 at grid point downstream of stagnation region

$$h_\beta \cos\gamma = \frac{(vF_x - uF_y)(\partial y/\partial\beta) + (wF_x - uF_z)(\partial z/\partial\beta)}{F_x V} \tag{10}$$

In the present study, Instead of the streamline metrics, the parameter of hd_β is calculated. This parameter is the perpendicular distance between adjacent streamlines (Dyakonov and DeJarnette, 2003). It can be calculated using a neighbor streamline. This neighbor streamline is started from a location near the starting point (which heating rate is needed on it) and is traced back to the stagnation point. The scale factor at a node like p_i, as indicated in Figure 7, multiplied by d_β would be the distance between two streamlines that is perpendicular at node p_i (Dyakonov and DeJarnette, 2003). At any node like p_i, the parameter of $h_\beta d_\beta$ can be easily calculated, since it would be equal to the distance between p_i and p_n. Point p_n is a point on neighbor streamline with a s-distance equal to that of p_i. The parameter of hd_β now can be calculated, since $h_\beta d_\beta$ is known and angle γ can be determined using known coordinates of p_{i-1}, p_i, p_n:

$$hd_\beta = h_\beta d_\beta \sin(\gamma) \tag{11}$$

Since we calculate hd_β, replacing of body radius with hd_β would not cause any problem if d_β is constant along the streamline. This is true since β is constant along each streamline. As seen in Equations (4) and (7), the body radius, which should be replaced by h in axisymmetric analog, appears in nominator and denominator with the same power. Therefore the calculated value of hd_β can be used instead of metric coefficient. In this condition, Equations (4) and (7) are changed to the following equations, respectively:

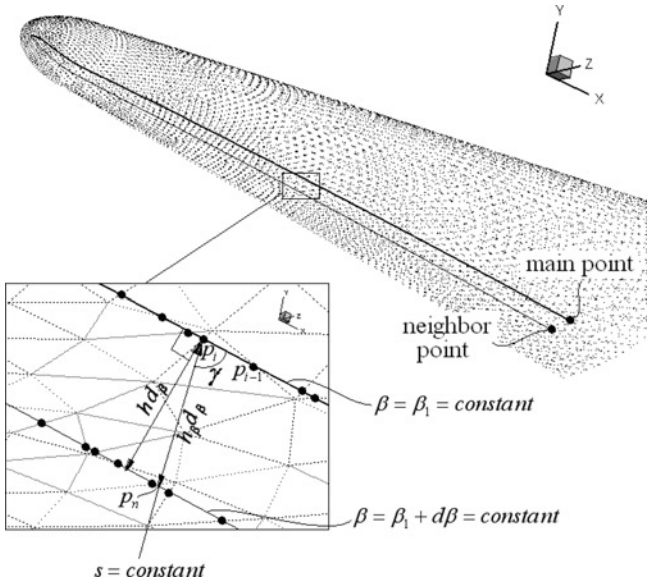

Figure 7.
Scale factor definition

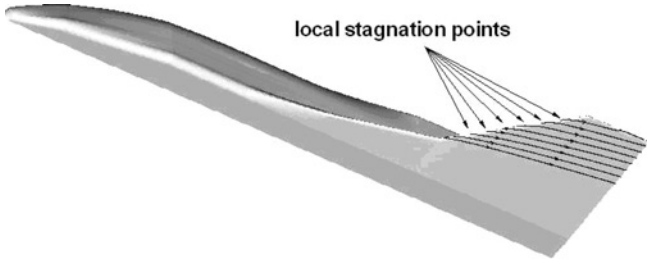

Figure 8.
Wing streamlines for a wing-body configuration

$$\theta_L = \frac{0.644\left[\int_0^s \rho^* \mu^* V_e (hd_\beta)^2 ds\right]^{1/2}}{\rho_e V_e h d_\beta} \tag{12}$$

$$\theta_T = \frac{c_2\left[\int_0^s \rho^* \mu^{*m} V_e (hd_\beta)^{c_3} ds\right]^{c_4}}{\rho_e V_e h d_\beta} \tag{13}$$

In complex 3-D geometries, some streamlines are not started from the nose stagnation point. For example in Figure 1, nose streamlines do not cover most of the wing surface. In fact, the streamlines on the wing have local stagnation points on the wing leading edge (Figure 8). Our scheme, in which streamlines are traced back, recognizes these local stagnations. The flow over the wing is nearly two dimensional and the Zoby's convective equations are also 2-D in the case of $h = 1$. Therefore, in the present technique, the metric coefficients are set equal to one along the streamlines which is initiated from the wing leading edge.

6. Results

In order to demonstrate the capability and accuracy of the present method, surface heating rates are calculated for laminar and turbulent conditions over 3-D wing-body configurations. As it was mentioned previously, any unstructured Euler code can be used to produce the required inviscid surface properties for the present method. The unstructured Euler code used in the present study is based on the Roe's flux splitting method [?]. Details about the number of grids and the solution will be given for each case.

6.1 Laminar flow over the elliptic cone (case 1)

The perfect gas, laminar flow over a blunted 2:1 elliptic cone is examined at angle of attack of 15 deg. The cone angles in the windward and side planes are 5 and 9.93 deg, respectively. The freestream conditions are $M_\infty = 10.19, \rho_\infty = 0.0193$ kg/m^3 and $T_\infty = 51.1$°K. The wall temperature is $T_w = 261$°K and the nose radius in the side plane is $R_n = 0.0254$ m. Since the flow is symmetric about the mid plane of vehicle, only half of the solution domain is considered for this analysis. About 70,000 cells are used to generate the unstructured grid needed for the inviscid solution. This grid includes 3,000 triangular cells on the body surface. It is noted that based on the numerical tests performed by the authors, grid independent results are obtained on this grid.

Surface heating rates calculated by the present method are compared with the results of the approximate method of Riley and DeJarnette (1992a, b), the thin layer NS method of Riley and DeJarnette (1992a, b) and the experimental data of Hillsamer and Rhudy (1964). Circumferential surface heating rates are depicted in Figures 9-11 at three axial locations on the body. Similar to the present method, the Riley's approximate method uses axisymmetric analog and Zoby's convective equations. However the approximation made in the inviscid solution limits the application of Riley's method to windward surface of the blunt cones. As it is shown, present results agree very well with the experimental data on both windward and leeward regions of the body. However, there are some discrepancies between the present results and the experimental data at the location of $x/R_n = 9.7$. This difference is also seen between

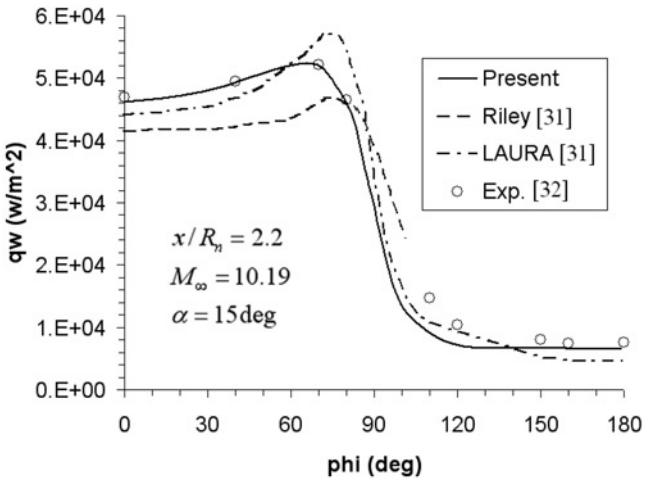

Figure 9.
Comparison of circumferential surface heating rates for 2:1 ellipsoidal cone at $x/R_n = 2.2$

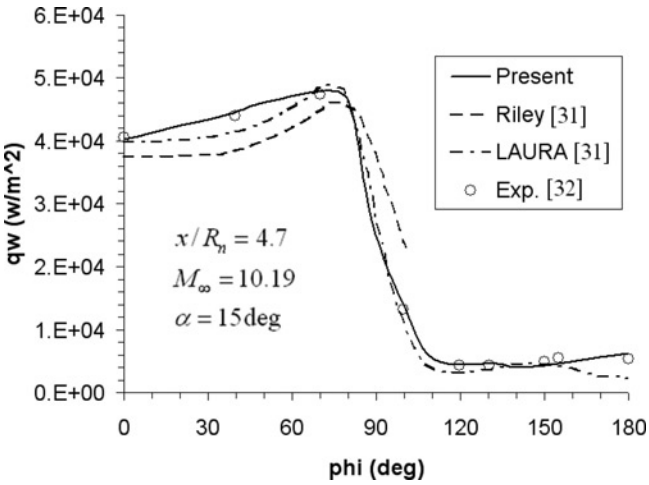

Figure 10.
Comparison of circumferential surface heating rates for 2:1 ellipsoidal cone at $x/R_n = 4.7$

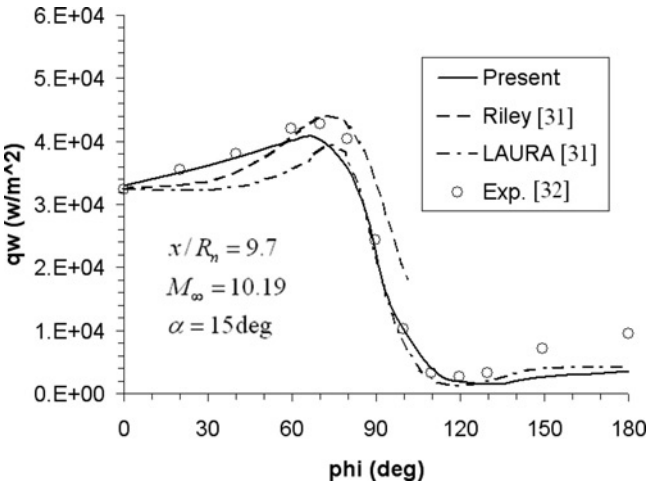

Figure 11.
Comparison of circumferential surface heating rates for 2:1 ellipsoidal cone at $x/R_n = 9.7$

the results from LAURA and the experimental data and perhaps it is because of some transitional flow effects in the downstream of the body.

6.2 Turbulent flow over the wing of X-15 hypersonic airplane (case 2)

The X-15 was a rocket-powered aircraft that was used by NASA to test hypersonic flight conditions in the 1960s. As is seen in Figure 12, it has a configuration with many three-dimensional details. The available experimental data of heating rates (Quinn and Olinger, 1969) over this airplane makes it a suitable case for comparison purposes. An unstructured grid with 194,000 cells is used to calculate the inviscid properties on the half part of the solution domain. The number of cells on the body surface is 30,000.

Turbulent heat transfer coefficients over windward and leeward regions of the wing midspan are compared with the flight data in this case. In this paper, geometry details of X-15 are taken from Quinn and Olinger (1969). Two sets of flight conditions are

considered. The first condition corresponds to $M_\infty = 5.1, \alpha = 2^\circ, P_\infty = 4{,}550$ Pa and $T_\infty = 217^\circ$K. For the wall temperature we have used its reported data in Quinn and Olinger (1969), which varies along the wing chord. Comparison of Stanton numbers along the wing chord are shown in Figures 13 and 14. Excellent agreement is seen between the present results and the flight data in both windward and leeward regions.

Second set of flight conditions corresponds to $M_\infty = 4.98, \alpha = 16.3^\circ, P_\infty = 2{,}540$ Pa and $T_\infty = 223^\circ$K. The wall temperature is variable and its value is read from the reported data in Quinn and Olinger (1969). Comparison of Stanton numbers along the wing chord are shown in Figures 15 and 16. In this case, some fluctuations are seen in the flight data, especially in the leeward region. This may be due to the turbulent effect in the high angle of attack conditions in this case. The present inviscid-boundary layer method, can not predict these fluctuations. However, the overall agreement between the present results and the flight data is good.

In the previous case, it was shown that the present method is capable of predicting the heating rates over complex geometries. The reason is that the present method can use the inviscid results of unstructured grids; a mesh which is suitable for modeling of

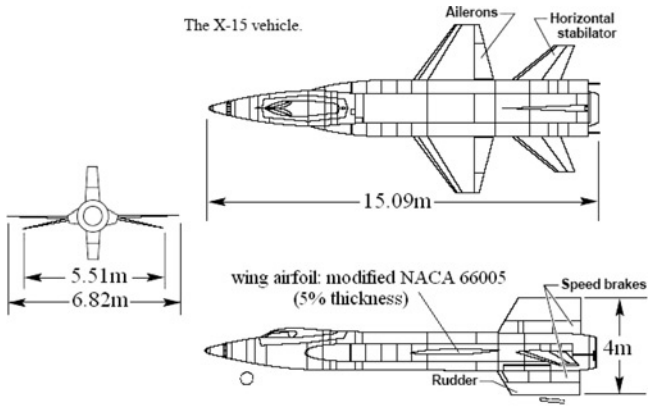

Figure 12.
View drawings of X-15 hypersonic aircraft

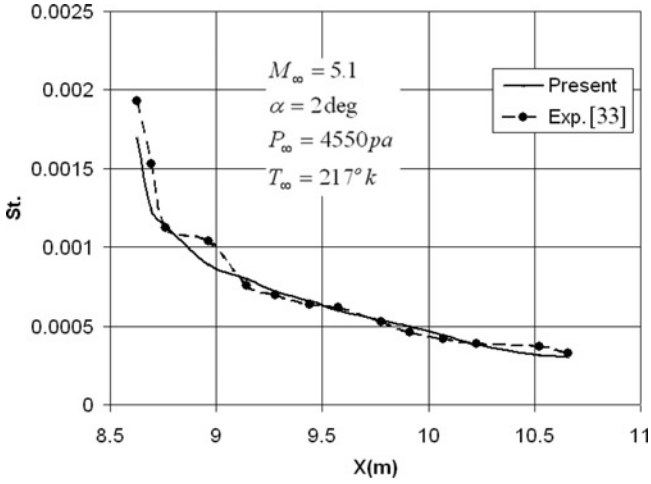

Figure 13.
Comparison of Stanton number on lower surface of X-15 wing for the first set of flight conditions

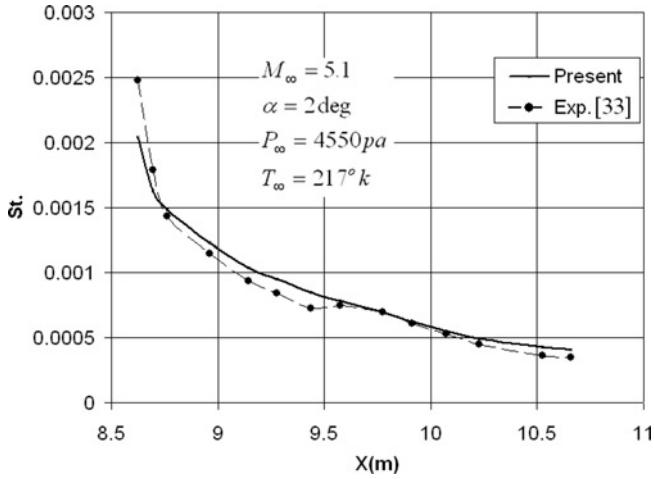

Figure 14.
Comparison of Stanton number on upper surface of X-15 wing for the first set of flight conditions

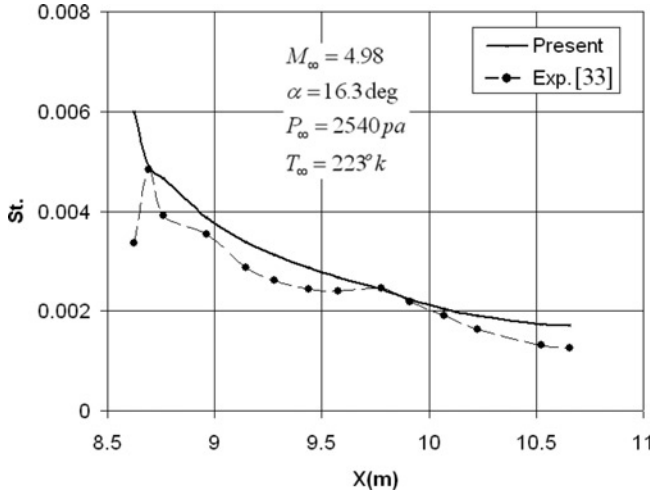

Figure 15.
Comparison of Stanton number on lower surface of X-15 wing for the second set of flight conditions

complex geometries. It should be noted that inviscid-boundary layer methods which use the approximate inviscid solution (Zoby *et al.*, 1981; Riley and DeJarnette, 1992a, b; Riley, 1992; Malekzadeh *et al.*, 2003; Maslen, 1964, 1971) are not able to predict heating rates over arbitrary complex geometries. Also low supersonic flows can not be studied with them. However the present method can easily calculate low supersonic heating rates over wing-body combinations. To demonstrate this, the wing section of a rocket-propelled model is considered in the next case.

6.3 Turbulent surface heating rates for the X-34 (case 3)
The X-34 is a reusable, sub-orbital test vehicle developed at NASA (Pamadi, *et al.*, 2000; Kleb *et al.*, 1998). As seen in Figure 17, its length is 17.6 m with a wing span of 8.46 m.

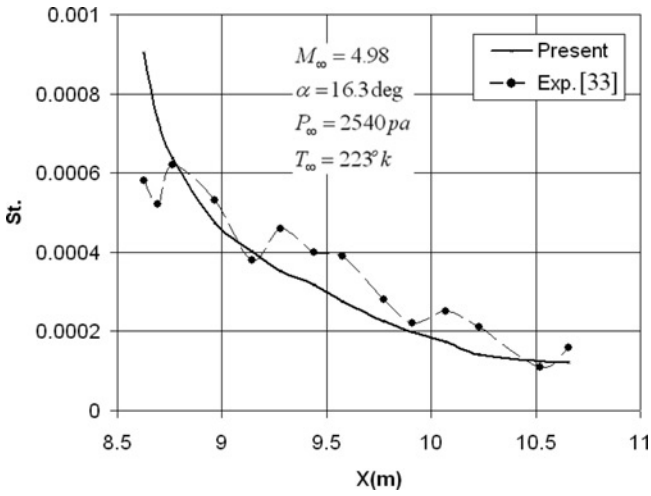

Figure 16.
Comparison of Stanton number on upper surface of X-15 wing for the second set of flight conditions

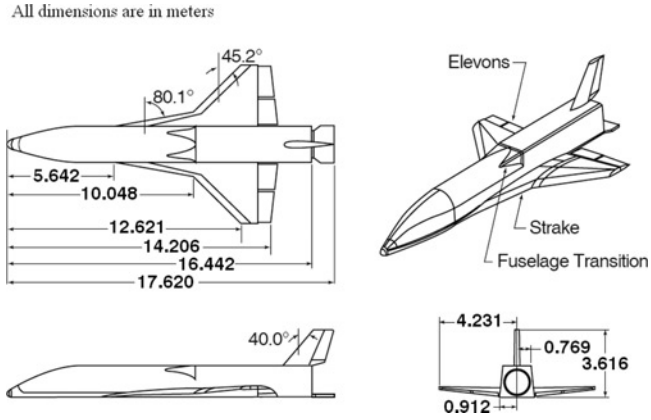

Figure 17.
View drawings of X-34

Surface heating rates are examined along the windward symmetry line, and three axial locations of this vehicle at $M_\infty = 6, \alpha = 15.22^\circ, P_\infty = 651$ Pa and $T_\infty = 234^\circ$K. The locations of these three cross-sectional cut planes are shown in Figure 18.

Aerodynamic heating of X-34 has been analyzed in NASA Langley Research Center using engineering code of LATCH (Pamadi *et al.*, 2000), and the full Navier-Stokes CFD code of LAURA (Kleb *et al.*, 1998). In Figure 19, turbulent heating rate distribution obtained from the present method at the windward symmetry plane is compared with the results of LATCH and LAURA. As it is seen, the present results are obtained on three different unstructured grids with 89,000, 201,000 and 524,000 cells. In each case, about 10 per cent of the cells are located on the body surfaces. The differences between results calculated on these three grids are very small and therefore the grid with 89,000 cells would be an appropriate grid for this calculation. In comparison with the LAURA code, the present method slightly overpredicts the heating rates at front part and underpredicts it at the rear part of X-34 windward symmetry plane. However the overall accuracy of the present results is better than the LATCH code and stays within

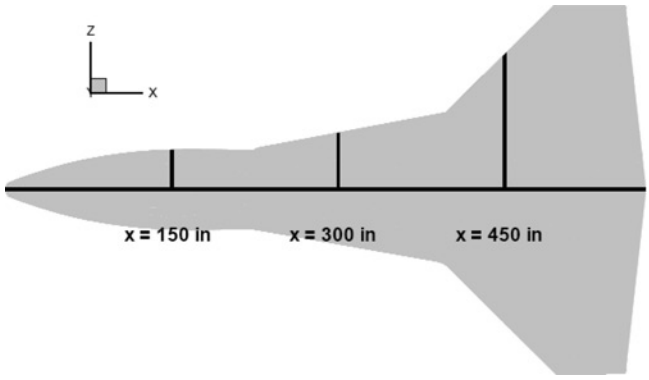

Figure 18.
Locations of three cross sectional cut planes

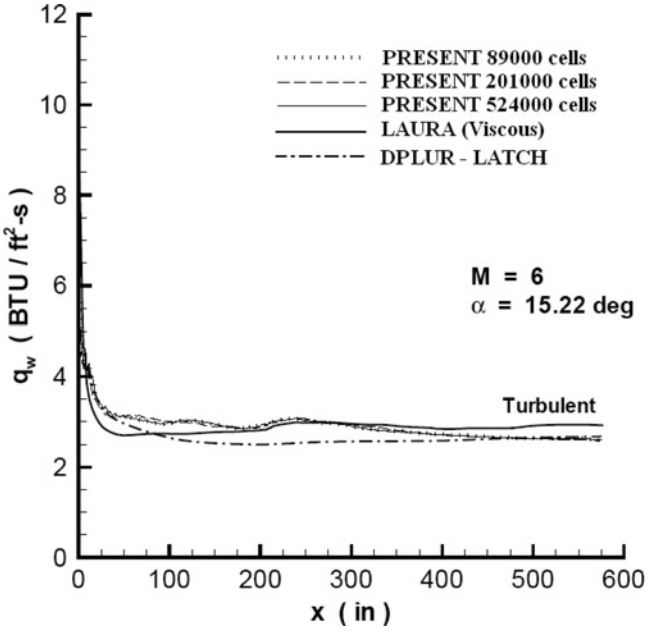

Figure 19.
Grid refinement results of turbulent heating distribution at windward centerline on X-34

15 per cent of LAURA code. The difference between the present results and LATCH code is because of the different methods used for metric coefficients. Also probable small different inviscid results may cause some differences between two results.

In Figures 20-22, turbulent heating rates are compared with Langley's results on a grid with 89,000 cells. Having considered the complexities in the geometry of X-34, the present method predicts reasonably good surface heating rates. In comparison with the LATCH code, the present results in windward plane are in better agreement with the results of LAURA code.

The required inviscid properties of the present method are obtained from an Euler solution. Therefore total CPU time for this method is more than the CPU time required

in the methods which use approximate inviscid solution. However, the total CPU time of the present method is still much less than the CPU time of a full Navier-Stokes solution. Therefore on complex geometries, where engineering methods using approximate inviscid solutions are not applicable, the present method has advantages in comparison to full Navier-Stokes solution, when talking about CPU time. The reasonably accurate results of present method for 3-D vehicles make this method an excellent design tool for hypersonic prediction of aerodynamic heating.

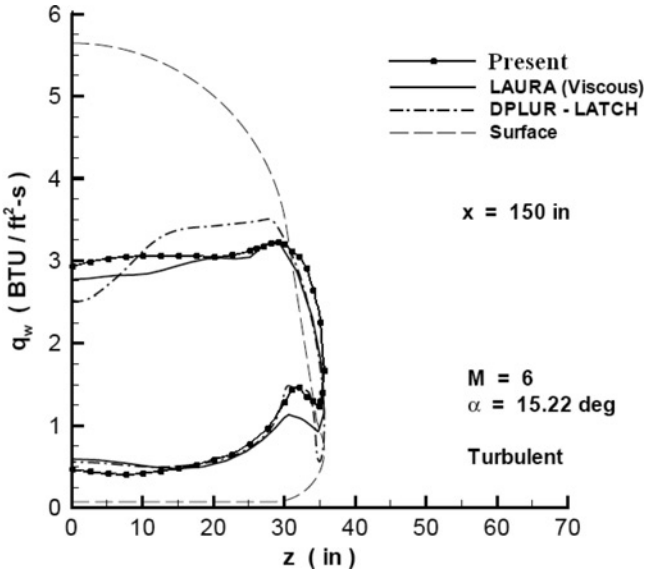

Figure 20.
Lateral turbulent heating distribution on X-34 at x = 3.81 m

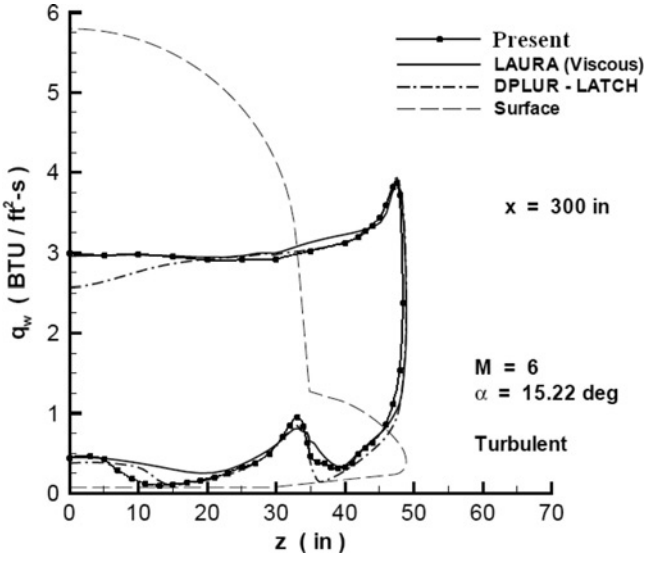

Figure 21.
Lateral turbulent heating distribution on X-34 at x = 7.62 m

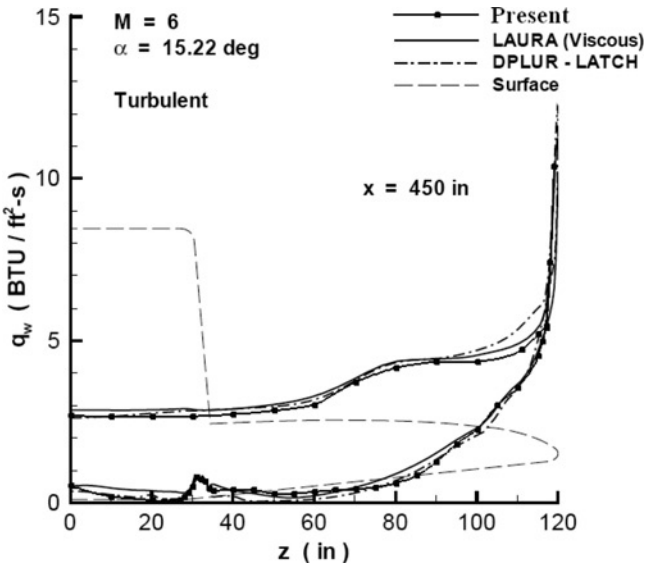

Figure 22.
Lateral turbulent heating distribution on X-34 at x = 11.43 m

7. Conclusion

A procedure for evaluating surface heating rates for three-dimensional non-axisymmetric geometries at angle of attack is developed. This axisymmetric analog based procedure uses three-dimensional inviscid properties calculated on an unstructured grid to trace streamlines, and uses Zoby's approximate convective-heating equations for heating rate computation. A simple technique is also presented to calculate the metric coefficient for general cases. The procedure is applied to the prediction of heating rates over 3-D bodies and wing configurations. Good agreements are obtained between predictions and experimental data in both windward and leeward regions of different complex geometries of wing-body combinations in the absence of flow separation.

References

Anderson, J.D. (1989), *Hypersonic and High Temperature Gas Dynamics*, McGraw-Hill Book Company, New York, NY.

Cooke, J.C. (1961), *An Axially Symmetric Analogue for General Three-dimensional Boundary Layers*, Aeronautical Research Council TR R&M 3200, British Ministry of Aviation.

DeJarnette, F.R. and Davis, R.M. (1968), "A simplified method for calculating laminar heat transfer over bodies at an angle of attack of attack", NASA TN D-4720.

DeJarnette, F.R. and Hamilton, H.H. (1973), "Inviscid surface streamlines and heat transfer on shuttle-type configurations", *Journal of Spacecraft and Rockets*, Vol. 10 No. 5, pp. 314-21.

DeJarnette, F.R., Hamilton, H.H., Weilmuenster, K.J. and Cheatwood, F.M. (1978), "A review of some approximate methods used in aerodynamic heating analysis", *Journal of Thermo Physics*, Vol. 1 No. 1, pp. 5-12.

Dyakonov, A.A. and DeJarnette, F.R. (2003), "Streamlines and aerodynamic heating for unstructured grids on high speed vehicles", AIAA paper 2003-151.

Eckert, E.R.G. (1955), "Engineering relations for friction and heat transfer to surfaces in high velocity flow", *Journal of the Aeronautical Sciences*, Vol. 22 No. 8, pp. 585-7.

Hamilton, H.H., DeJarnette, F.R. and Weilmuenster, K.J. (1987), "Application of axisymmetric analog for calculating heating in three-dimensional flows", *Journal of Spacecraft and Rockets*, Vol. 24 No. 4, pp. 296-302.

Hamilton, H.H., Greene, F.A. and DeJarnette, F.R. (1993), "An approximate method for calculating heating rates on three-dimensional vehicles", AIAA paper 93-2881.

Hamilton, H.H., Weilmuenster, K.J. and DeJarnette, F.R. (2006), "Improved approximate method for computing convective heating on hypersonic vehicles using unstructured grids", 9th AIAA/ASME Joint Thermophysics and Heat Transfer Conference, 5-8 June 2006, San Francisco, CA, AIAA 2006-3394.

Hansen, C.F. (1958), "Approximations for the thermodynamic and transport properties of high-temperature air", NASA TN-4150.

Hillier, R. and Soltani, S. (1995), "Navier–Stokes computations of hypersonic flows", *International Journal of Numerical Methods for Heat & Fluid Flow*, Vol. 5 No. 3, pp. 195-211.

Hillsamer, M.E. and Rhudy, J.P. (1964), "Heat-transfer and shadowgraph tests of several elliptical lifting bodies at Mach 10", AEDC-TDR 64-19, US Air Force.

Johnson, C.B. and Bushnell, D.M. (1970), "Power-Law velocity-profile-exponent variations with Reynolds number, wall cooling, and Mach number in a turbulent boundary layer", NASA TN D-5753.

Karimian, S.M.H. and Mahdizadeh, A. (2001), "Approximate solution of inviscid flow around the nose of hypersonic bodies at angle of attack", *Amirkabir Journal*, Vol. 12 No. 47, pp. 35-47.

Kleb, W.L., Wood, W.A., Gnoffo, P.A. and Alter, S.J. (1998), "Computational aeroheating predictions for X-34", AIAA paper 98-0779.

Malekzadeh, M., Karimian, S.M.H. and Marefat, M. (2003), "An engineering inviscid-boundary layer method for calculation of aerodynamic heating in the leeward region", *Proceedings of CFD2003, 11th Annual Conference of the CFD Society of Canada, Vancouver*.

Maslen, S.H. (1964), "Inviscid hypersonic flow past smooth symmetric bodies", *AIAA Journal*, Vol. 2 No. 6, pp. 1055-61.

Maslen, S.H. (1971), "Asymmetric hypersonic flow", NASA CR-2123.

Mehta, R.C. (2000), "Heat transfer study of high speed flow over a spiked blunt body", *International Journal of Numerical Methods for Heat & Fluid Flow*, Vol. 10 No. 7, pp. 750-69.

Mulas, M., Chibbaro, S., Delussu, G., Piazza, I.D. and Talice, M. (2002), "Efficient parallel computations of flows of arbitrary fluids for all regimes of Reynolds, Mach and Grashof numbers", *International Journal of Numerical Methods for Heat & Fluid Flow*, Vol. 12 No. 6, pp. 637-57.

Pamadi, B.N., Brauckmann, G.J., Ruth, M.J. and Fuhrmann, H.D. (2000), "Aerodynamic characteristics, database development and flight simulation of the X-34 vehicle", AIAA paper 2000-0900.

Parhizkar, H. and Karimian, S.M.H. (2006), "Laminar and turbulent aeroheating predictions around multi-cone configurations in hypersonic equilibrium-air flow", *JAST Journal of Aerospace Science and Technology*, Vol. 3 No. 3, pp. 159-66.

Quinn, R.D. and Olinger, F.V. (1969), "Heat-transfer measurements obtained on the X-15 airplane including correlations with wind-tunnel results", NASA TM X-1750.

Riley, C.J. (1992), "An engineering method for interactive inviscid-boundary layer in three-dimensional hypersonic flow", PhD thesis, North Carolina State University, Raleigh, NC.

Riley, C.J. and DeJarnette, F.R. (1990), "An approximate method for calculation three-dimensional inviscid hypersonic flow fields", NASA TP-3018.

Riley, C.J. and DeJarnette, F.R. (1991), "Engineering calculations of three-dimensional inviscid hypersonic flow fields", *Journal of Spacecraft and Rockets*, Vol. 28, pp. 628-35.

Riley, C.J. and DeJarnette, F.R. (1992a), "Engineering aerodynamic heating method for hypersonic flow", *Journal of Spacecraft and Rockets*, Vol. 2, pp. 327-34.

Riley, C.J. and DeJarnette, F.R. (1992b), "An engineering aerodynamic heating method for hypersonic flow", AIAA 92-0499.

Riley, C.J., Kleb, W.L. and Alter, S.J. (1998), "Aeroheating predictions for X-34 using an inviscid-boundary layer method", AIAA paper 98-0880.

Simeonides, G. (1998), "Generalized reference enthalpy formulations and simulation of viscous effects in hypersonic flow", *Shock Waves*, Vol. 8 No. 3, pp. 161-72.

Soltani, S., Morgan, K. and Peraire, J. (1993), "an upwind unstructured grid solution algorithm for compressible flow", *International Journal of Numerical Methods for Heat & Fluid Flow*, Vol. 3 No. 4, pp. 283-304.

Tannehill, J.C. and Mugge, P.H. (1974), "Improved curve fits for the thermodynamic properties of equilibrium air suitable for numerical computer using time-dependent or shock-capturing methods", NASA CR-2470.

White, F.M. (1974), *Viscous Fluid Flow*, McGraw-Hill Book Company, New York, NY.

Zoby, E.V., Moss, J.J. and Sutton, K. (1981), "Approximate convective-heating equations for hypersonic flows", *Journal of Spacecraft and Rockets*, Vol. 18 No. 1, pp. 64-70.

Corresponding author
H. Parhizkar can be contacted at: hparhiz@aut.ac.ir; hparhiz@yahoo.com